

LASERS

https://doi.org/10.1070/QEL16391

Analytical model of a transversely diode-pumped alkali metal vapour laser

A.I. Parkhomenko, A.M. Shalagin

Abstract. **The previously presented analytical model of a transversely diode-pumped alkali metal vapour laser (A.I. Parkhomenko, A.M. Shalagin, *Quantum Electronics*, 2015, Vol. 45, No. 9, pp 797–806) is refined and expanded. Analytical formulas are derived describing the operation of a high-intensity laser at an almost arbitrary buffer gas pressure and taking into account radiation losses in the resonator. Comparison of the results of calculations of the laser energy characteristics by analytical formulas with the results of numerical calculations of other authors shows very good agreement.**

Keywords: *alkali metal vapour laser, diode pumping, collisions.*

1. Introduction

In recent years, diode-pumped alkali metal vapour lasers have been intensively investigated experimentally and theoretically [1–5]. A great interest in these lasers is reasonably associated with their ability to generate cw radiation of very high power, while demonstrating a high conversion efficiency of pump radiation into laser radiation.

The maximum output of an alkali metal vapour laser has been achieved in work [4], where the creation of a longitudinally diode-pumped caesium vapour laser with closed-cycle laser-active medium circulation is reported. In cw mode, the laser radiation power was 1 kW with a conversion efficiency of pump energy into laser energy amounting to 48%.

Obtaining significantly higher powers requires the scaling of the process. In our opinion, the geometry with transverse pumping is optimal for scaling. In this geometry, the power of the generated radiation increases in proportion to the length of the laser. The idea of a transversely diode-pumped alkali metal vapour laser was patented [6] and first implemented in [7]. A theoretical model of such a laser was first proposed by Komashko and Zweiback [8]. The laser operation was described in [8] by a rather complex system of differential equations, which was solved numerically in the approximation of the effective absorption cross section of pump radiation. Yang et al. [9] developed a somewhat different numerical model of the laser than that presented in work [8]. The equations in [9] were solved numerically on the assumption that the population levels of the atoms of the active medium do not depend on the coordinate along the resonator axis, i.e., they are constant along the propagation direction of the laser output.

In paper [10], we developed an analytical model of a transversely diode-pumped alkali metal vapour laser, which describes the operation of the laser in the practically important case of high radiation intensity but at a sufficiently high buffer gas pressure and in the absence of radiation loss in the resonator. The aim of the present paper is to expand the analytical model [10] for the possibility of describing the generation of a high-intensity laser at an almost arbitrary buffer gas pressure and taking into account radiation losses in the resonator.

2. Equations describing the operation of a laser

An alkali metal vapour laser operates in accordance with a three-level scheme (Fig. 1). The laser cycle includes optical excitation of the D_2 ($^2S_{1/2}$–$^2P_{3/2}$) transition, the population of the $^2P_{1/2}$ level in collisions of alkali metal atoms at the $^2P_{3/2}$ level with the buffer gas particles, and laser generation at the D_1 ($^2P_{1/2}$–$^2S_{1/2}$) transition. In Fig. 1, the levels $^2S_{1/2}$, $^2P_{1/2}$ and $^2P_{3/2}$ are denoted by figures 1, 2 and 3, respectively.

Let us consider the operation of a transversely diode-pumped alkali metal vapour laser. The scheme of the laser is shown in Fig. 2. To simplify the analysis, we assumed that a cell with alkali metal vapours and buffer gases has the form

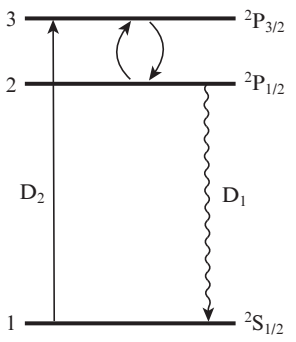

Figure 1. Diagram of energy levels and transitions in alkali metal atoms. The straight line shows the transition caused by pump radiation, the wavy line corresponds to the laser transition and curved lines indicate collisional transitions.

A.I. Parhomenko Institute of Automation and Electrometry, Siberian Branch, Russian Academy of Sciences, prosp. Akad. Koptyuga 1, 630090 Novosibirsk, Russia; e-mail: par@iae.nsk.su;
A.M. Shalagin Institute of Automation and Electrometry, Siberian Branch, Russian Academy of Sciences, prosp. Akad. Koptyuga 1, 630090 Novosibirsk, Russia; Novosibirsk State University, ul. Pirogova 2, 630090 Novosibirsk, Russia; e-mail: shalagin@iae.nsk.su

Received 28 March 2017
Kvantovaya Elektronika **47** (8) 683–692 (2017)
Translated by I.A. Ulitkin

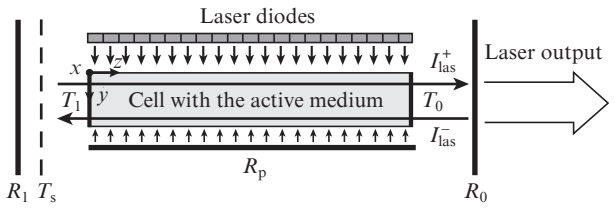

Figure 2. Scheme of a transversely diode-pumped alkali metal vapour laser.

of a rectangular parallelepiped with edges z_0 (length), y_0 (width) and x_0 (height). Pump laser diodes are arranged on one side of the cell. Their radiation enters the cell in the xz plane and propagates in the y direction. For a more efficient utilisation of the pump energy, a plane mirror is mounted on the other side of the cell, which reflects the pump radiation passing through it (the reflection coefficient of the mirror, R_p) back to the cell. The resonator consists of two plane mirrors with reflection coefficients R_0 and R_1. The transmission coefficients of the cell windows are T_0 and T_1. The radiation energy losses in the resonator (due to the diffraction of light at the edges of the mirrors, due to the geometric imperfection of the resonator, due to the scattering of light in the medium by inhomogeneities) are taken into account by introducing the effective transmittance T_s. The value of T_s characterises the relative losses of the radiation energy in the resonator in one pass, excluding the transmission losses of the windows. It is assumed that the losses of T_s are localised in front of the rear mirror R_1. Laser radiation is coupled out of the cell in the xy plane through a semitransparent mirror with a reflection coefficient R_0 and propagates in the z direction. For simplicity, we assume that the intensity distribution of pump radiation is uniform in the xz plane (at the input to the cell). In this case, as a consequence, the intensity distribution of laser radiation is also uniform along the height of the cell (along the x axis).

Under steady-state conditions, absorption of pump radiation and amplification of laser radiation are described by the equations:

$$\frac{\partial I^{\pm}_{\omega p}(y,z,\omega)}{\partial y} = \mp\Big[N_1(y,z) - \frac{1}{2}N_3(y,z)\Big]\sigma_p(\omega) I^{\pm}_{\omega p}(y,z,\omega),$$
$$\frac{\partial I^{\pm}_{las}(y,z)}{\partial z} = \mp[N_1(y,z) - N_2(y,z)]\sigma_{las}(\omega_{las}) I^{\pm}_{las}(y,z). \quad (1)$$

Here, $I^+_{\omega p}(y,z,\omega)$ and $I^-_{\omega p}(y,z,\omega)$ are the spectral densities of the pump radiation power at a frequency ω, propagating along the y axis and in the opposite direction (after reflection by the mirror), respectively; $I^+_{las}(y,z)$ and $I^-_{las}(y,z)$ are the intensities of laser radiation propagating along the z axis and in the opposite direction, respectively; $N_1(y,z)$, $N_2(y,z)$ and $N_3(y,z)$ are the populations of levels 1, 2 and 3; $\sigma_p(\omega)$ is the absorption cross section of pump radiation; and $\sigma_{las}(\omega_{las})$ is the absorption cross section of laser radiation with frequency ω_{las}. The absorption cross sections are found from the formulas:

$$\sigma_p(\omega) = \frac{\lambda_p^2 A_{31}}{2\pi}\frac{\Gamma_p}{\Gamma_p^2 + (\omega - \omega_{31})^2},$$
$$\sigma_{las}(\omega_{las}) = \frac{\lambda_{las}^2 A_{21}}{4\pi}\frac{\Gamma_{las}}{\Gamma_{las}^2 + (\omega_{las} - \omega_{21})^2}, \quad (2)$$

where λ_p and λ_{las} are the centre wavelengths of pump radiation and laser radiation; A_{31} and A_{21} are the spontaneous emission rates (the first Einstein coefficients) for 3–1 and 2–1 transitions; $\Gamma_p = A_{31}/2 + \gamma_{31}$ and $\Gamma_{las} = A_{21}/2 + \gamma_{21}$ are the homogeneous half-widths of 3–1 and 2–1 transition lines, respectively; γ_{31} and γ_{21} are the collision half-widths of 3–1 and 2–1 transition lines; ω_{31} and ω_{21} are the frequencies of 3–1 and 2–1 transitions. Equations (1) are supplemented by boundary conditions describing the change in radiation intensities on the mirror surface in the course of reflection and propagation through the cell windows:

$$I^+_{\omega p}(0,z,\omega) = I_{0\omega p}(\omega),$$
$$I^-_{\omega p}(y_0,z,\omega) = R_p I^+_{\omega p}(y_0,z,\omega),$$
$$I^+_{las}(y,0) = R_1 T_1^2 T_s^2 I^-_{las}(y,0), \quad (3)$$
$$I^-_{las}(y,z_0) = R_0 T_0^2 I^+_{las}(y,z_0).$$

The populations of levels 1, 2 and 3 in equations (1) are found from the balance equations. In the steady-state case, these equations have the form:

$$w_p(y,z)\Big[N_1(y,z) - \frac{1}{2}N_3(y,z)\Big] - (A_{31} + \nu_{31} + \nu_{32})N_3(y,z) + \nu_{23}N_2(y,z) = 0,$$
$$w_{las}(y,z)[N_1(y,z) - N_2(y,z)] - (A_{21} + \nu_{21} + \nu_{23})N_2(y,z) + \nu_{32}N_3(y,z) = 0, \quad (4)$$
$$N_1(y,z) + N_2(y,z) + N_3(y,z) = N.$$

Here, N is the total concentration of active atoms; collision frequencies ν_{32} and ν_{23} describe collisional mixing between levels 3 and 2; collision frequencies ν_{31} and ν_{21} describe inelastic collision transitions along the $3 \to 1$ and $2 \to 1$ channels; and $w_p(y,z)$ and $w_{las}(y,z)$ are the probabilities of induced transitions under the action of pump radiation and generated laser radiation, respectively. We assume that pump radiation has a spectrum of arbitrary width, and generated laser radiation is monochromatic. Then

$$w_p(y,z) = \int_0^\infty \frac{\sigma_p(\omega)}{\hbar\omega_p} I_{\omega p}(y,z,\omega)\,d\omega,$$
$$w_{las}(y,z) = \frac{\sigma_{las}(\omega_{las})}{\hbar\omega_{las}} I_{las}(y,z), \quad (5)$$

where ω_p is the centre frequency of the pump radiation spectrum; and

$$I_{\omega p}(y,z,\omega) = I^+_{\omega p}(y,z,\omega) + I^-_{\omega p}(y,z,\omega),$$
$$I_{las}(y,z) = I^+_{las}(y,z) + I^-_{las}(y,z) \quad (6)$$

is the total spectral power density of pump radiation inside the cell and the total intensity of laser radiation inside the cell, respectively. The collision frequencies ν_{32} and ν_{23}, due to the principle of detailed balance, are related by the expressions

$$\nu_{23} = 2\nu_{32}\xi, \quad \xi \equiv \exp\Big(-\frac{\Delta E}{k_B T}\Big), \quad (7)$$

where $\Delta E = \hbar\omega_{32}$ is the energy difference between levels 3 and 2; and T is the temperature of the gas mixture inside the cell.

From the system of algebraic equations (4) we find the populations of levels:

$$\begin{aligned}
N_2(y,z) &= N\Big(\frac{\varkappa_p\nu_{32}}{\nu_{32}+3\Gamma_2/2}+\frac{\varkappa_{las}\Gamma_3}{\nu_{23}+2\Gamma_3}+\frac{b\varkappa_p\varkappa_{las}}{4}\Big)\\
&\times(1+\varkappa_p+\varkappa_{las}+b\varkappa_p\varkappa_{las})^{-1},\\
N_3(y,z) &= N\Big(\frac{\varkappa_p\Gamma_2}{\nu_{32}+3\Gamma_2/2}+\frac{\varkappa_{las}\nu_{23}}{\nu_{23}+2\Gamma_3}+\frac{b\varkappa_p\varkappa_{las}}{2}\Big)\\
&\times(1+\varkappa_p+\varkappa_{las}+b\varkappa_p\varkappa_{las})^{-1},\\
N_1(y,z) &= N\Big(1+\frac{\varkappa_p\Gamma_2}{2\nu_{32}+3\Gamma_2}+\frac{\varkappa_{las}\Gamma_3}{\nu_{23}+2\Gamma_3}+\frac{b\varkappa_p\varkappa_{las}}{4}\Big)\\
&\times(1+\varkappa_p+\varkappa_{las}+b\varkappa_p\varkappa_{las})^{-1},
\end{aligned} \tag{8}$$

and population differences characterising laser generation and pump absorption:

$$\begin{aligned}
N_2(y,z)-N_1(y,z) &= N\frac{a\varkappa_p-1}{1+\varkappa_p+\varkappa_{las}+b\varkappa_p\varkappa_{las}},\\
N_1(y,z)-\frac{1}{2}N_3(y,z) &= N\frac{1+q\varkappa_{las}}{1+\varkappa_p+\varkappa_{las}+b\varkappa_p\varkappa_{las}},
\end{aligned} \tag{9}$$

where

$$\begin{aligned}
&\Gamma_2=\tilde{A}_{21}+\nu_{23};\quad \Gamma_3=\tilde{A}_{31}+\nu_{32};\\
&\tilde{A}_{21}=A_{21}+\nu_{21};\quad \tilde{A}_{31}=A_{31}+\nu_{31};\\
&a=\frac{(1-\xi)\nu_{32}-\tilde{A}_{21}/2}{(1+3\xi)\nu_{32}+3\tilde{A}_{21}/2};\quad q=\frac{(1-\xi)\nu_{32}+\tilde{A}_{31}}{2[(1+\xi)\nu_{32}+\tilde{A}_{31}]};\\
&b=\frac{(\tilde{A}_{21}+2\xi\tilde{A}_{31})\nu_{32}+\tilde{A}_{21}\tilde{A}_{31}}{[(1+\xi)\nu_{32}+\tilde{A}_{31}][(1+3\xi)\nu_{32}+3\tilde{A}_{21}/2]};
\end{aligned} \tag{10}$$

$\tilde{A}_{31}$ and $\tilde{A}_{21}$ are the transition frequencies from levels 3 and 2 as a result of spontaneous emission and collisional transitions to the ground state; and Γ_3 and Γ_2 are the total transition frequencies from levels 3 and 2 as a result of spontaneous emission and collisions. The quantities $\varkappa_p \equiv \varkappa_p(y,z)$ and $\varkappa_{las} \equiv \varkappa_{las}(y,z)$ are defined as

$$\begin{aligned}
&\varkappa_p=\frac{w_p(y,z)}{\beta_p},\quad \varkappa_{las}=\frac{w_{las}(y,z)}{\beta_{las}},\\
&\beta_p=\frac{(\tilde{A}_{21}+2\xi\tilde{A}_{31})\nu_{32}+\tilde{A}_{21}\tilde{A}_{31}}{(1+3\xi)\nu_{32}+3\tilde{A}_{21}/2},\\
&\beta_{las}=\frac{(\tilde{A}_{21}+2\xi\tilde{A}_{31})\nu_{32}+\tilde{A}_{21}\tilde{A}_{31}}{2[(1+\xi)\nu_{32}+\tilde{A}_{31}]}.
\end{aligned} \tag{11}$$

They denote the saturation parameters, since each of them characterises the degree of population equalisation at the 3–1 or 2–1 transition in the absence of the second field.

Taking into account relations (9), differential equations (1), describing the operation of the laser, have the form:

$$\begin{aligned}
\frac{\partial I^{\pm}_{\omega p}(y,z,\omega)}{\partial y} &= \mp\frac{(1+q\varkappa_{las})N\sigma_p(\omega)I^{\pm}_{\omega p}(y,z,\omega)}{1+\varkappa_p+\varkappa_{las}+b\varkappa_p\varkappa_{las}},\\
\frac{\partial I^{\pm}_{las}(y,z)}{\partial z} &= \pm\frac{(a\varkappa_p-1)N\sigma_{las}(\omega_{las})I^{\pm}_{las}(y,z)}{1+\varkappa_p+\varkappa_{las}+b\varkappa_p\varkappa_{las}}.
\end{aligned} \tag{12}$$

As follows from the equations for $I^{\pm}_{las}$ in (12), lasing occurs when the condition $a\varkappa_p > 1$ is fulfilled. To ensure effective generation ($a\varkappa_p \gg 1$), one must meet the conditions

$$\nu_{32} \gg \tilde{A}_{21}, \tilde{A}_{31},\quad \varkappa_p \gg \frac{1+3\xi}{1-\xi}. \tag{13}$$

The first condition in (13) is satisfied with a large margin at a sufficiently high pressure of the buffer gas (~1 atm and higher). To fulfil the second condition, the spectral power density of pump radiation must be sufficiently high. Under these conditions, pumping produces an extremely large population inversion at the laser transition.

3. Relationship between integral characteristics of radiations

The system of differential equations (12) describing the laser operation can be solved only by numerical methods. Nevertheless, it is possible, without solving it, to obtain a practically important relationship between the integral characteristics of radiations.

We will show how this relationship directly follows from Eqns (12). Integrating the difference between the third (for I^{+}_{las}) and fourth (for I^{-}_{las}) equations in (12) over the cell volume (with respect to x, y, z), taking into account formulas (5) and (11) for w_{las} and $\varkappa_{las}$, for the output power of laser radiation coupled out of the cell

$$P_{out} = x_0\int_0^{y_0}[I^{+}_{las}(y,z_0)-I^{-}_{las}(y,z_0)+I^{-}_{las}(y,0)-I^{+}_{las}(y,0)]\,dy \tag{14}$$

we obtain an expression

$$P_{out} = N\hbar\omega_{las}\beta_{las}x_0\int_0^{z_0}dz\int_0^{y_0}dy\,\frac{\varkappa_{las}(a\varkappa_p-1)}{1+\varkappa_p+\varkappa_{las}+b\varkappa_p\varkappa_{las}}. \tag{15}$$

Hereafter, we assume that in the considered geometry of the transversely pumped laser, laser radiation is generated in the entire cell volume $V = x_0y_0z_0$.

The intensity $I^{out}_{las}(y)$ of laser radiation emerging from the resonator through a semitransparent mirror with a reflection coefficient R_0 is given by the expression

$$I^{out}_{las}(y) = T_0(1-R_0)I^{+}_{las}(y,z_0). \tag{16}$$

The output power P^{out}_{las} of laser radiation emerging from the resonator through a semitransparent mirror is defined as the integral of the intensity over the beam cross section:

$$P^{out}_{las} = x_0\int_0^{y_0}I^{out}_{las}(y)\,dy. \tag{17}$$

Let us find the relationship between the powers P^{out}_{las} (17) and P_{out} (15). From the last two equations in (12) we obtain the expression

$$\frac{1}{I^{+}_{las}(y,z)}\frac{\partial I^{+}_{las}(y,z)}{\partial z} = -\frac{1}{I^{-}_{las}(y,z)}\frac{\partial I^{-}_{las}(y,z)}{\partial z}, \tag{18}$$

from which it follows that the product $I^+_{las}(y,z)I^-_{las}(y,z)$ does not depend on z. In particular, the relation

$$I^+_{las}(y,z_0)I^-_{las}(y,z_0) = I^+_{las}(y,0)I^-_{las}(y,0) \tag{19}$$

is valid. The integrand in (14), taking into account (16), (19) and boundary conditions (3), has the form

$$I^+_{las}(y,z_0) - I^-_{las}(y,z_0) + I^-_{las}(y,0) - I^+_{las}(y,0) = \frac{I^{out}_{las}(y)}{R}, \tag{20}$$

where

$$R = \frac{T_0(1-R_0)\sqrt{\tilde{R}_l}}{(\sqrt{\tilde{R}_0}+\sqrt{\tilde{R}_l})(1-\sqrt{\tilde{R}_0\tilde{R}_l})};$$
$$\tilde{R}_0 = R_0T_0^2; \quad \tilde{R}_l = R_lT_l^2T_s^2; \tag{21}$$

Expressions (14), (15), (17) and (20) yield the relationship between the powers P^{out}_{las} and P_{out} (15):

$$P^{out}_{las} = RP_{out} = RN\hbar\omega_{las}\beta_{las}x_0 \times\int_0^{z_0}dz\int_0^{y_0}dy\,\frac{\varkappa_{las}(a\varkappa_p-1)}{1+\varkappa_p+\varkappa_{las}+b\varkappa_p\varkappa_{las}}. \tag{22}$$

Let us write the difference between the second (for $I^-_{\omega p}$) and first (for $I^+_{\omega p}$) equations in (12) and integrate it with respect to the frequency ω. Taking into account formulas (5) and (11) for w_p and $\varkappa_p$, we obtain an expression

$$\frac{\partial I^-_p(y,z)}{\partial y} - \frac{\partial I^+_p(y,z)}{\partial y} = \frac{N\hbar\omega_p\beta_p\varkappa_p(1+q\varkappa_{las})}{1+\varkappa_p+\varkappa_{las}+b\varkappa_p\varkappa_{las}}, \tag{23}$$

where

$$I^\pm_p(y,z) = \int_0^\infty I^\pm_{\omega p}(y,z,\omega)\,d\omega \tag{24}$$

are the total intensities of pump radiation propagating along the y axis (the superscript '+') and in the opposite direction (after reflection by the mirror, the superscript '–'). Integrating equation (23) over the cell volume, we obtain for the absorbed pump power

$$P_{abs} = x_0\int_0^{z_0}[I^+_p(0,z) - I^+_p(y_0,z) + I^-_p(y_0,z) - I^-_p(0,z)]dz \tag{25}$$

an expression

$$P_{abs} = N\hbar\omega_p\beta_px_0\int_0^{z_0}dz\int_0^{y_0}dy\,\frac{\varkappa_p(1+q\varkappa_{las})}{1+\varkappa_p+\varkappa_{las}+b\varkappa_p\varkappa_{las}}. \tag{26}$$

Below we will take into account that the total losses of the pump power for spontaneous emission and collisional quenching in the cell volume are given by a fairly obvious relationship:

$$P_{loss} = \hbar\omega_px_0\int_0^{z_0}dz\int_0^{y_0}[N_2(y,z)\tilde{A}_{21} + N_3(y,z)\tilde{A}_{31}]dy. \tag{27}$$

Taking into account formulas (8) for the population levels, expression (27) has the form

$$P_{loss} = N\hbar\omega_px_0 \times\int_0^{z_0}dz\int_0^{y_0}dy\,\frac{\beta_p\varkappa_p+\beta_{las}\varkappa_{las}+\varkappa_p\varkappa_{las}b(\tilde{A}_{21}+2\tilde{A}_{31})/4}{1+\varkappa_p+\varkappa_{las}+b\varkappa_p\varkappa_{las}}. \tag{28}$$

From (22), (26), and (28) we obtain the expression

$$P^{out}_{las} = R\frac{\omega_{las}}{\omega_p}(P_{abs}-P_{loss}), \tag{29}$$

relating the output power P^{out}_{las} of laser radiation coupled out from the resonator with the absorbed pump power P_{abs} and the pump power losses P_{loss} due to spontaneous emission and collisional quenching.

The pump power loss P_{loss} during the laser operation arises both due to the loss of spontaneous emission and collisional quenching and due to the unabsorbed pump power

$$P_{unabs} = P_{0p} - P_{abs}, \tag{30}$$

where P_{0p} is the pump power at the entrance to the cell. Taking this relation into account, formula (29) for the laser radiation power can also be represented in the form

$$\frac{P^{out}_{las}}{P_{0p}} = R\frac{\omega_{las}}{\omega_p}\left(1-\frac{P_{unabs}+P_{loss}}{P_{0p}}\right). \tag{31}$$

The ratio of the laser power to the pump power, P^{out}_{las}/P_{0p}, characterises the efficiency of the conversion of pump radiation into laser radiation, and the ratio of radiation frequencies ω_{las}/ω_p is the quantum efficiency of this conversion. For alkali metal vapours it is close to unity (95% for caesium, 98% for rubidium and 99.5% for potassium), which ensures a high efficiency of alkali metal vapour lasers. The conversion efficiency of pump radiation into laser radiation P^{out}_{las}/P_{0p} the higher, the smaller the relative total pump power losses $(P_{unabs}+P_{loss})/P_{0p}$.

4. High intensity of laser radiation

The system of differential equations (12) describing the laser operation can be solved in general only numerically. In our previous work [10], an analytical solution of Eqn (12) was obtained for the case of high laser radiation intensity and a sufficiently high buffer gas pressure, which is reduced to the fulfilment of conditions

$$\varkappa_{las} \gg 1+\varkappa_p+b\varkappa_p\varkappa_{las}, \quad \varkappa_{las} \gg 1/q. \tag{32}$$

The first condition means both a high intensity of laser radiation (a large saturation parameter $\varkappa_{las}$, not only in comparison with unity, but also in comparison with a saturation parameter for pump radiation $\varkappa_p$) and a high pressure ensuring a small parameter b such that $b\varkappa_p \ll 1$. In order to satisfy the second condition in (32), a sufficiently large saturation parameter $\varkappa_{las}$ (in particular, for rubidium atoms $1/q \approx 5$) is also needed.

In paper [10], based on approximation (32), we left in equation (12) only $\varkappa_{las}$ in the denominator and discarded unity in the first equation of (12) in the numerator in comparison with $q\varkappa_{las}$. As a result, the equations were greatly simplified and an analytical solution was obtained.

In the present paper we remove the strict restriction $b\varkappa_p \ll 1$ and find out the influence of the term $b\varkappa_p\varkappa_{las}$ in the denominators of equations (12) on the lasing characteristics at not very high buffer gas pressures. Instead of restrictions (32), we impose weaker restrictions:

$$(1+b\varkappa_p)\varkappa_{las} \gg 1+\varkappa_p, \quad q\varkappa_{las} \gg 1, \quad b\varkappa_p \lesssim 1. \tag{33}$$

When conditions (33) are satisfied, differential equations (12) have the form:

$$\frac{\partial I^{\pm}_{\omega p}(y,\omega)}{\partial y} = \mp\, qN\sigma_p(\omega)\,\frac{I^{\pm}_{\omega p}(y,\omega)}{1+b\varkappa_p(y)},$$
$$\frac{\partial I^{\pm}_{las}(y,z)}{\partial z} = \pm N\beta_{las}\hbar\omega_{las}\,\frac{a\varkappa_p(y)-1}{1+b\varkappa_p(y)}\,\frac{I^{\pm}_{las}(y,z)}{I^{+}_{las}(y,z)+I^{-}_{las}(y,z)}, \tag{34}$$

where the saturation parameter $\varkappa_p$ is independent of the coordinate z and is given, in accordance with (5), (6), (11), by the expression

$$\varkappa_p(y) = \frac{1}{\beta_p\hbar\omega_p}\int_0^{\infty}\sigma_p(\omega)[I^{+}_{\omega p}(y,\omega)+I^{-}_{\omega p}(y,\omega)]\,d\omega. \tag{35}$$

Solving the equations for the laser radiation intensities in (34) with allowance for the boundary conditions (3), we obtain the expression for $I^{\pm}_{las}$:

$$I^{\pm}_{las}(y,z) = \frac{I_{las}(y,z)}{2} \pm \frac{N}{2}\beta_{las}\hbar\omega_{las}\frac{a\varkappa_p(y)-1}{1+b\varkappa_p(y)} \times\left[z - z_0\frac{(1-\tilde R_l)\sqrt{\tilde R_0}}{(\sqrt{\tilde R_0}+\sqrt{\tilde R_l})(1-\sqrt{\tilde R_0\tilde R_l})}\right], \tag{36}$$

where $I_{las}(y,z)$ is the total intensity of laser radiation inside the cell, determined by the formula

$$I_{las}(y,z) \equiv I^{+}_{las}(y,z)+I^{-}_{las}(y,z) = N\beta_{las}\hbar\omega_{las}\frac{a\varkappa_p(y)-1}{1+b\varkappa_p(y)} \times\left\{\left[z - z_0\frac{(1-\tilde R_l)\sqrt{\tilde R_0}}{(\sqrt{\tilde R_0}+\sqrt{\tilde R_l})(1-\sqrt{\tilde R_0\tilde R_l})}\right]^2 + z_0^2\frac{4\tilde R_0\tilde R_l}{(\sqrt{\tilde R_0}+\sqrt{\tilde R_l})^2(1-\sqrt{\tilde R_0\tilde R_l})^2}\right\}^{1/2}. \tag{37}$$

If the effective reflection coefficients of the mirrors, $\tilde R_l$ and $\tilde R_0$, are close to unity, then, according to (37), the laser radiation intensity I_{las} inside the cell is almost constant along the z axis of the resonator. From formulas (16) and (36) we find the laser output intensity

$$I^{out}_{las}(y) = RNz_0\beta_{las}\hbar\omega_{las}\frac{a\varkappa_p(y)-1}{1+b\varkappa_p(y)}, \tag{38}$$

where R is given by the formula in (21).

Next, to solve the problem, we need to find the saturation parameter $\varkappa_p(y)$, determined by the first two equations for the spectral power densities of pump radiation $I^{\pm}_{\omega p}(y,\omega)$ in (34). We will solve these equations by the method of successive approximations with respect to the small quantity $b\varkappa_p$. For $b = 0$ (zeroth approximation), the first two equations in (34) have the form [10]:

$$\frac{\partial I^{\pm(0)}_{\omega p}(y,\omega)}{\partial y} = \mp qN\sigma_p(\omega)I^{\pm(0)}_{\omega p}(y,\omega). \tag{39}$$

According to [10], the solution of equations (39), taking into account boundary conditions (3), is given by the expressions

$$I^{+(0)}_{\omega p}(y,\omega) = I_{0\omega p}(\omega)\exp[-qN\sigma_p(\omega)y],$$
$$I^{-(0)}_{\omega p}(y,\omega) = R_pI_{0\omega p}(\omega)\exp[-qN\sigma_p(\omega)(2y_0-y)]. \tag{40}$$

In the next approximation, the first two equations in (34) have the form

$$\frac{\partial I^{\pm(1)}_{\omega p}(y,\omega)}{\partial y} = \mp\frac{qN\sigma_p(\omega)I^{\pm(1)}_{\omega p}(y,\omega)}{1+b\varkappa^{(0)}_p(y)}, \tag{41}$$

where the initial approximate value of the saturation parameter $\varkappa^{(0)}_p$ is given by the expression

$$\varkappa^{(0)}_p(y) = \frac{1}{\beta_p\hbar\omega_p}\int_0^{\infty}\sigma_p(\omega)[I^{+(0)}_{\omega p}(y,\omega)+I^{-(0)}_{\omega p}(y,\omega)]\,d\omega. \tag{42}$$

The solution of equations (41) with allowance for boundary conditions (3) is given by the expression:

$$I^{+(1)}_{\omega p}(y,\omega) = I_{0\omega p}(\omega)\exp[-qN\sigma_p(\omega)\varphi(y)],$$
$$I^{-(1)}_{\omega p}(y,\omega) = R_pI_{0\omega p}(\omega)\exp\{qN\sigma_p(\omega)[\varphi(y)-2\varphi(y_0)]\}, \tag{43}$$
$$\varphi(y) = \int_0^{y}\frac{dy}{1+b\varkappa^{(0)}_p(y)}.$$

As the final expression for the saturation parameter $\varkappa_p$, we have the expression obtained on the basis of relation (43):

$$\varkappa_p(y) = \frac{1}{\beta_p\hbar\omega_p}\int_0^{\infty}\sigma_p(\omega)[I^{+(1)}_{\omega p}(y,\omega)+I^{-(1)}_{\omega p}(y,\omega)]\,d\omega. \tag{44}$$

Thus, formulas (38) and (44) describe the operation of a diode-pumped alkali metal vapour laser in the practically important case of a sufficiently high intensity of laser radiation and a weak restriction from below on the buffer gas pressure (for $b\varkappa_p \lesssim 1$).

5. Analysis of lasing characteristics

To further define the calculations using the above formulas, it is necessary to specify the spectral power density $I_{0\omega p}(\omega)$ of the pump diodes at the cell input. We assume that at the input to the cell the pump radiation spectrum is Gaussian:

$$I_{0\omega p}(\omega) = \frac{I_{0p}}{\sqrt{\pi}\,\Delta\omega}\exp\left[-\left(\frac{\omega-\omega_p}{\Delta\omega}\right)^2\right],$$
$$I_{0p} = \int_0^{\infty}I_{0\omega p}(\omega)\,d\omega, \tag{45}$$

where I_{0p} is the pump radiation intensity at the cell input; and $\Delta\omega$ is the half-width (at the level 1/e) of the pump radiation spectrum.

From (43), taking into account (45) for the total spectral power density $I_{\omega p}(y,\omega)$ of pump radiation inside the cell, we obtain the relation

$$I_{\omega p}(y,\omega) = I^{+(1)}_{\omega p}(y,\omega)+I^{-(1)}_{\omega p}(y,\omega) = \frac{I_{0p}}{\sqrt{\pi}\,\Delta\omega}\{\exp[-g(\omega,y)]+R_p\exp[g(\omega,y)-2g(\omega,y_0)]\}, \tag{46}$$
$$g(\omega,y) = \left(\frac{\omega-\omega_p}{\Delta\omega}\right)^2 + q\sigma_p(\omega)N\varphi(y).$$

The saturation parameter $\varkappa_p^{(0)}(y)$ (42) that appears in the formula for the function $\varphi(y)$ is given by the expression

$$\varkappa_p^{(0)}(y) = \frac{\varkappa_0}{\sqrt{\pi}\,\Delta\omega} \times \int_0^\infty \frac{\exp[-g_0(\omega,y)] + R_p \exp[g_0(\omega,y) - 2g_0(\omega,y_0)]}{1 + [(\omega-\omega_{31})/\Gamma_p]^2}\,\mathrm{d}\omega, \quad (47)$$

$$\varkappa_0 = \frac{\sigma_p(\omega_{31}) I_{0p}}{\beta_p \hbar \omega_p}, \quad g_0(\omega,y) = \left(\frac{\omega-\omega_p}{\Delta\omega}\right)^2 + q\sigma_p(\omega) N y.$$

Using (46), we find the total intensity of pump radiation inside the cell:

$$I_p(y) = \int_0^\infty I_{\omega p}(y,\omega)\,\mathrm{d}\omega = \frac{I_{0p}}{\sqrt{\pi}\,\Delta\omega} \times \int_0^\infty \{\exp[-g(\omega,y)] + R_p \exp[g(\omega,y) - 2g(\omega,y_0)]\}\,\mathrm{d}\omega. \quad (48)$$

The saturation parameters $\varkappa_p(y)$ and $\varkappa_{las}(y,z)$ under the conditions in question are given by the expressions:

$$\varkappa_p(y) = \frac{\varkappa_0}{\sqrt{\pi}\,\Delta\omega} \times \int_0^\infty \frac{\exp[-g(\omega,y)] + R_p \exp[g(\omega,y) - 2g(\omega,y_0)]}{1 + [(\omega-\omega_{31})/\Gamma_p]^2}\,\mathrm{d}\omega, \quad (49)$$

$$\varkappa_{las}(y,z) = \frac{\sigma_{las}(\omega_{las})}{\beta_{las}\hbar\omega_{las}} I_{las}(y,z).$$

For the laser output power, from expression (17), using (38), we obtain

$$P_{las}^{out} = RNx_0 z_0 \beta_{las} \hbar \omega_{las} \int_0^{y_0} \frac{a\varkappa_p(y) - 1}{1 + b\varkappa_p(y)}\,\mathrm{d}y. \quad (50)$$

Note here the following important circumstance. Analysis shows that on the right-hand side of formula (50) the concentration N of active particles and cell width y_0 enter only in the combination Ny_0. This means that, under the condition Ny_0 = const, the change in the cell width does not affect the laser output power P_{las}^{out}.

For the pump power losses due to spontaneous emission and collisional quenching in the cell volume, from (28), when conditions (33) are satisfied, we find the expression

$$P_{loss} = N\hbar\omega_p x_0 z_0 \int_0^{y_0} \frac{\beta_{las} + (b/4)(\tilde{A}_{21} + 2\tilde{A}_{31})\varkappa_p(y)}{1 + b\varkappa_p(y)}\,\mathrm{d}y. \quad (51)$$

For the absorbed pump power in the cell volume, from expression (26), when conditions (33) are satisfied, we obtain the expression

$$P_{abs} = Nq\hbar\omega_p \beta_p x_0 z_0 \int_0^{y_0} \frac{\varkappa_p(y)}{1 + b\varkappa_p(y)}\,\mathrm{d}y. \quad (52)$$

We will calculate the energy characteristics of the laser using the formulas given above. Let the active medium in the laser cell be rubidium atoms, and a mixture of helium and methane be used as a buffer gas. Methane is usually used for effective collisional mixing between excited levels 3 and 2 in alkali metal atoms [1]. Helium is added to increase the collisional broadening of the D_2 line in order to make more efficient use of broadband emission from pump diodes [1].

We specify the initial parameters required for the calculation. For rubidium atoms, according to the NIST database [11], the rates of radiative transitions are $A_{21} = 3.6\times10^7$ s^{-1}, $A_{31} = 3.8\times10^7$ s^{-1}, transition wavelengths are $\lambda_{21} = 794.8$ nm, $\lambda_{31} = 780.0$ nm and the energy difference ΔE between levels 3 and 2 is 237.6 cm^{-1}. Collisional broadening for rubidium atoms in a helium buffer gas is as follows [12]: $\gamma_{He(D_1)} = 9.45$ MHz Torr^{-1} for the D_1 line and $\gamma_{He(D_2)} = 10.0$ MHz Torr^{-1} for the D_2 line. For rubidium atoms in a methane buffer gas, collisional broadening is as follows [12]: $\gamma_{CH_4(D_1)} = 14.55$ MHz Torr^{-1} for the D_1 line and $\gamma_{CH_4(D_2)} = 13.1$ MHz Torr^{-1} for the D_2 line.

To find the collision frequency ν_{32}, we used the following cross sections for the collisional transitions between the fine components of the excited state of rubidium atoms: $\sigma_{32(He)} = 0.103\times10^{-16}$ cm^2 for rubidium atoms in helium [13] and $\sigma_{32(CH_4)} = 42\times10^{-16}$ cm^2 for rubidium atoms in methane [14]. Because of the small cross section $\sigma_{32(He)}$, a molecular gas is added to the buffer mixture.

For the cross sections $\sigma_{31(CH_4)}$ and $\sigma_{21(CH_4)}$ of the collisional quenching of excited levels 3 and 2 of rubidium atoms interacting with methane, Zameroski et al. [15] experimentally obtained values not exceeding 1.9×10^{-18} cm^2. In calculating collision frequencies ν_{31} and ν_{21}, we assumed that $\sigma_{31(CH_4)} = \sigma_{21(CH_4)} = 1.9\times10^{-18}$ cm^2. For rubidium atoms colliding with helium atoms, the collisional quenching cross sections are extremely small ($\sigma_{31(He)}$, $\sigma_{21(He)} \leqslant 3\times10^{-20}$ cm^2 [16]), and therefore quenching due to interaction with helium can be neglected.

We assume below in the calculation that the centre frequency of the pump radiation spectrum and the laser radiation frequency coincide with the frequencies of 3–1 and 2–1 transitions, respectively: $\omega_p = \omega_{31}$, $\omega_{las} = \omega_{21}$. The cell should be designed in such a way that the alkali metal vapour enters it through the side branches so that the concentration N of active particles inside the cell is set by the temperature of these branches containing an alkali metal and is not related to the temperature T of the gas mixture inside the cell.

We first consider the effect of the correction associated with the term $b\varkappa_p$ in the denominators of equations (34) on the lasing characteristics. This correction should be taken into account at not very high pressures of the buffer gas, when the parameter $b\varkappa_p$ is not too small. In the case of a sufficiently high buffer gas pressure, the parameter $b\varkappa_p$ is very small ($b\varkappa_p \ll 1$) and can be neglected in Eqns (34) (we can assume $b = 0$). In this case, $\varkappa_p(y) = \varkappa_p^{(0)}(y)$ and the analytical formulas given above, which describe lasing, coincide with the formulas obtained previously in [10] (it should be noted that in [10] we neglected the energy losses in the resonator, which are taken into account in this paper by introducing the transmission coefficients T_0 and T_1 of the cell windows and the effective transmittance T_s, which differ from unity).

Figure 3 shows the results of calculations using formula (50) (with a correction for the parameter $b\varkappa_p$ and without it) for the conversion efficiency of pump radiation into laser radiation P_{las}^{out}/P_{0p} (pump radiation power $P_{0p} = x_0 z_0 I_{0p}$) as a function of the helium buffer gas pressure p_{He} at different values of the parameter Ny_0 (the number of active atoms in the cell in a gas column of width y_0 with a unit cross section). The methane buffer gas pressure p_{CH_4} was assumed fixed and equal to 0.1 atm. Condition (33) of applicability of formula (50)

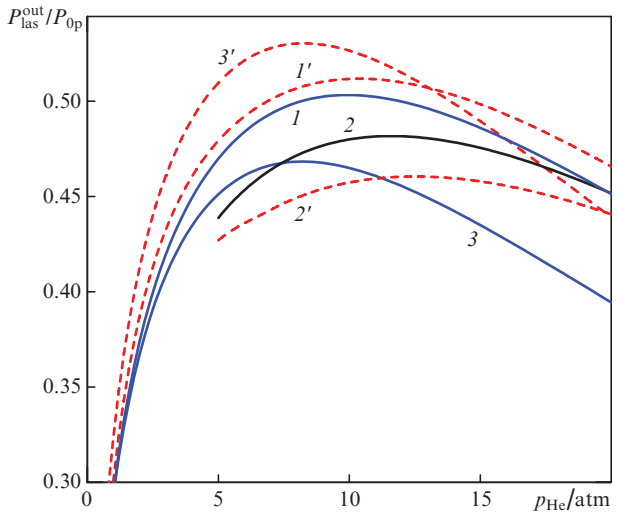

Figure 3. Effect of the parameter Ny_0 on the conversion efficiency. The calculation parameters are $I_{0p} = 3$ kW cm^{-2}, $\Delta\omega/(2\pi c) = 3$ cm^{-1}, $T = 395$ K, $p_{CH_4} = 0.1$ atm, $R_p = 0.99$, $R_0 = 0.3$, $R_1 = 0.99$, $T_0 = 0.99$, $T_1 = 0.99$, $T_s = 0.99$, $\omega_p = \omega_{31}$, $\omega_{las} = \omega_{21}$; (*1*, *1′*) $Ny_0 = 13.5\times10^{13}$, (*2*, *2′*) 18×10^{13} and (*3*, *3′*) 9×10^{13} cm^{-2}. Solid curves are the results of calculation in the first approximation in the parameter $b\varkappa_p$, dashed curves – calculation in the approximation $b = 0$.

with the parameters corresponding to Fig. 3 is met if the cell is sufficiently long (if $z_0 \gg y_0$). Thus, for example, for the parameters corresponding to curve (*1*) in Fig. 3, as well as for $z_0 = 10y_0$ and $p_{He} = 10$ atm [a maximum on curve (*1*)], relations $(1 + b\varkappa_p)\varkappa_{las} \geqslant 14(1 + \varkappa_p)$, $q\varkappa_{las} \geqslant 29$, $b\varkappa_p \leqslant 0.53$ hold true. It is clear from Fig. 3 that the conversion efficiency P_{las}^{out}/P_{0p} depends monotonically on the pressure p_{He} and the parameter Ny_0 and reaches a maximum value $(P_{las}^{out}/P_{0p})_{max}$ at some optimal helium pressure p_{He}^{opt} and some optimal parameter $(Ny_0)_{opt}$. If the parameter Ny_0 deviates from the optimal value [it corresponds to curve (*1*) in Fig. 3] in the direction of its increase [curve (*2*)] or decrease [curve (*3*)], the laser efficiency decreases dramatically. As can be seen from Fig. 3, the allowance for the correction for the parameter $b\varkappa_p$ can both reduce [cf. curves (*1*) and (*1′*), (*3*) and (*3′*)] and increase [cf. curves (*2*) and (*2′*)] the calculated values of P_{las}^{out}/P_{0p}. The effect of the correction on the calculated value of P_{las}^{out}/P_{0p} is small for the optimal value of the parameter Ny_0 [cf. curves (*1*) and (*1′*)] and becomes significant when Ny_0 deviates from the optimum value [cf. curves (*2*) and (*2′*), (*3*) and (*3′*)].

Let us consider in more detail the effect of the correction on the calculated value P_{las}^{out}/P_{0p} at the optimal value of the parameter Ny_0. At a helium pressure $p_{He} = 10$ atm, the calculated values of P_{las}^{out}/P_{0p} with correction for the parameter $b\varkappa_p$ [curve (*1*)] and without correction [curve (*1′*)] are 0.503 and 0.512, respectively, i.e., the relative change is 0.018. The parameter $b\varkappa_p(y)$ is a decreasing function of y. For the parameters corresponding to curve (*1*) in Fig. 3, and at a pressure $p_{He} = 10$ atm, we have $b\varkappa_p(0) = 0.530$ and $b\varkappa_p(y_0) = 0.268$. Thus, with the optimal value of the parameter Ny_0, the correction for the parameter $b\varkappa_p$ leads to a relative change in the conversion efficiency P_{las}^{out}/P_{0p} by an amount much smaller than the parameter $b\varkappa_p$ itself. Let us explain this somewhat surprising fact on the basis of the dependences of the laser radiation intensity on the coordinate y. Then, the reason for a more significant difference of curves (*2′*) and (*3′*) from (*2*) and (*3*) in Fig. 3 becomes clear.

The correction for the parameter $b\varkappa_p$ has a much stronger effect on the local laser radiation intensity. Figure 4 shows the laser radiation intensity $I_{las}^{out}(y)$ as a function of the coordinate y along the cell width for the parameters corresponding to curves (*1*) and (*1′*) in Fig. 3 and for a helium pressure $p_{He} = 10$ atm. It can be seen that taking the correction into account leads to a smoother dependence of $I_{las}^{out}(y)$: the intensity decreases from one side of the cell (at $y = 0$) and increases from the other side (at $y = y_0$). Relative changes in intensity near the two sides of the cell have different signs and turn out to be of the order of magnitude of $b\varkappa_p$. Note here the following circumstance. The laser radiation power P_{las}^{out} is an integral characteristic (17), i.e., it is proportional to the area under curves (*1*) and (*1′*) in Fig. 4. The difference in the areas under these curves characterises the effect of the correction for the parameter $b\varkappa_p$ on the calculated value of the laser radiation power. As a result, we see that locally the influence of the parameter $b\varkappa_p$ is quite appreciable, but for the integral characteristic P_{las}^{out} it is strongly suppressed due to the proximity of the areas under the curves. In the case of pairs of curves (*2*) and (*2′*), (*3*) and (*3′*) in Fig. 3, the situation is such that for the corresponding values of the parameter Ny_0, the dependences, similar to those in Fig. 4, give comparable differences between both local (with and without $b\varkappa_p$) and integral values of power.

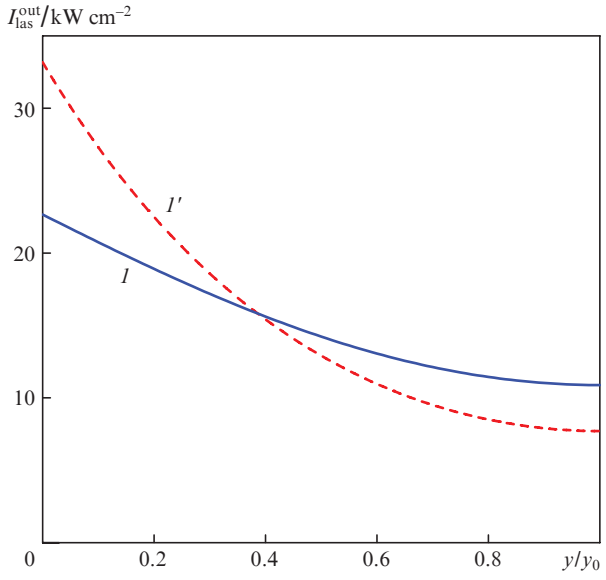

Figure 4. Laser radiation intensity $I_{las}^{out}(y)$ as a function of the y coordinate. The calculation parameters are $I_{0p} = 3$ kW cm^{-2}, $\Delta\omega/(2\pi c) = 3$ cm^{-1}, $T = 395$ K, $p_{He} = 10$ atm, $p_{CH_4} = 0.1$ atm, $Ny_0 = 13.5\times10^{13}$ cm^{-2}, $z_0 = 10y_0$, $R_p = 0.99$, $R_0 = 0.3$, $R_1 = 0.99$, $T_0 = 0.99$, $T_1 = 0.99$, $T_s = 0.99$, $\omega_p = \omega_{31}$, $\omega_{las} = \omega_{21}$. Curve (*1*) shows the results of calculation in the first approximation in the parameter $b\varkappa_p$, curve (*1′*) – calculation in the approximation $b = 0$.

Methane is added to the buffer mixture for rapid collisional mixing between upper levels 3 and 2 in the alkali metal atoms so that at a not too high buffer gas pressure the first effective generation condition is satisfied in (13) ($\nu_{32} \gg \tilde{A}_{21}, \tilde{A}_{31}$). The influence of the pressure of the methane buffer gas on the conversion efficiency of pump radiation into laser radiation at optimum values of the parameter Ny_0 is illustrated in Fig. 5. It can be seen that the addition of methane to the buffer mixture significantly improves the conversion efficiency and

greatly reduces the optimum helium pressure p_{He}^{opt}, at which the efficiency P_{las}^{out}/P_{0p} reaches its maximum value. Thus, in the absence of methane in the buffer mixture, the maximum efficiency $(P_{las}^{out}/P_{0p})_{max} = 0.40$ is attained at a high helium pressure $p_{He}^{opt} = 18.9$ atm [curve (*1*) in Fig. 5], while an increase in methane pressure p_{CH_4} to 0.5 atm increases the efficiency maximum (up to 0.58), attained at a lower helium pressure $p_{He}^{opt} = 7.3$ atm [curve (*4*) in Fig. 5].

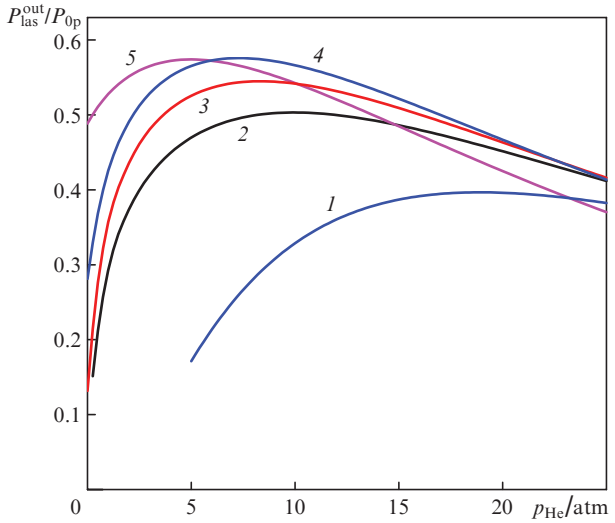

Figure 5. Effect of the methane buffer gas pressure p_{CH_4} on the conversion efficiency at optimum values of the parameter Ny_0. The calculation parameters are $I_{0p} = 3$ kW cm^{-2}, $\Delta\omega/(2\pi c) = 3$ cm^{-1}, $T = 395$ K, $R_p = 0.99$, $R_0 = 0.3$, $R_1 = 0.99$, $T_0 = 0.99$, $T_1 = 0.99$, $T_s = 0.99$, $\omega_p = \omega_{31}$, $\omega_{las} = \omega_{21}$; (*1*) $p_{CH_4} = 0$, $Ny_0 = 17.0\times10^{13}$ cm^{-2}, (*2*) $p_{CH_4} = 0.1$ atm, $Ny_0 = 13.5\times10^{13}$ cm^{-2}, (*3*) $p_{CH_4} = 0.2$ atm, $Ny_0 = 12.1\times10^{13}$ cm^{-2}, (*4*) $p_{CH_4} = 0.5$ atm, $Ny_0 = 10.8\times10^{13}$ cm^{-2} and (*5*) $p_{CH_4} = 2$ atm, $Ny_0 = 9.5\times10^{13}$ cm^{-2}.

The conversion efficiency P_{las}^{out}/P_{0p} depends monotonically on the helium pressure p_{He} and the parameter Ny_0 and reaches a maximum value $(P_{las}^{out}/P_{0p})_{max}$ at some optimal helium pressure p_{He}^{opt} and some optimal parameter $(Ny_0)_{opt}$. Figure 6 shows the results of calculations of the quantities $(P_{las}^{out}/P_{0p})_{max}$, p_{He}^{opt} and $(Ny_0)_{opt}$ as functions of methane pressure p_{CH_4} for two values of the intensity I_{0p} and half-width $\Delta\omega$ of the pump radiation spectrum chosen so that the spectral power density of pump radiation $I_{0p}/\Delta\omega$ remained unchanged. One can see from Fig. 6a that the maximum conversion efficiency is achieved at an optimum methane pressure $p_{CH_4}^{opt} = 0.5-1$ atm. Figure 6a also shows the calculated values of $(P_{las}^{out}/P_{0p})_{max}$ in approximation $b = 0$ [curves (*1′*) and (*2′*), for which the initial calculation parameters are the same as for curves (*1*) and (*2*), respectively]. It can be seen from a comparison of curves (*1*) and (*1′*), (*2*) and (*2′*) that at an optimum helium pressure p_{He}^{opt} and optimum parameter $(Ny_0)_{opt}$, the effect of correction for the parameter $b\varkappa_p$ on the calculated values of $(P_{las}^{out}/P_{0p})_{max}$ is small.

Consider the following important circumstance. Numerical analysis shows that for a given spectral power density of pump radiation $I_{0p}/\Delta\omega$ and selected optimal values of $p_{CH_4}^{opt}$, p_{He}^{opt} and $(Ny_0)_{opt}$ at different $\Delta\omega$, the lasing efficiency is the same (Fig. 6a). For example, the spectral power density of pump radiation is the same for curves (*1*) and (*2*) in Fig. 6a $(I_{0p}/[\Delta\omega/(2\pi c)] = 1$ kW cm^{-1}), and therefore for these curves the maximum of the ratio P_{las}^{out}/P_{0p} is the same and equal to 0.58 [at $p_{CH_4} \geqslant$

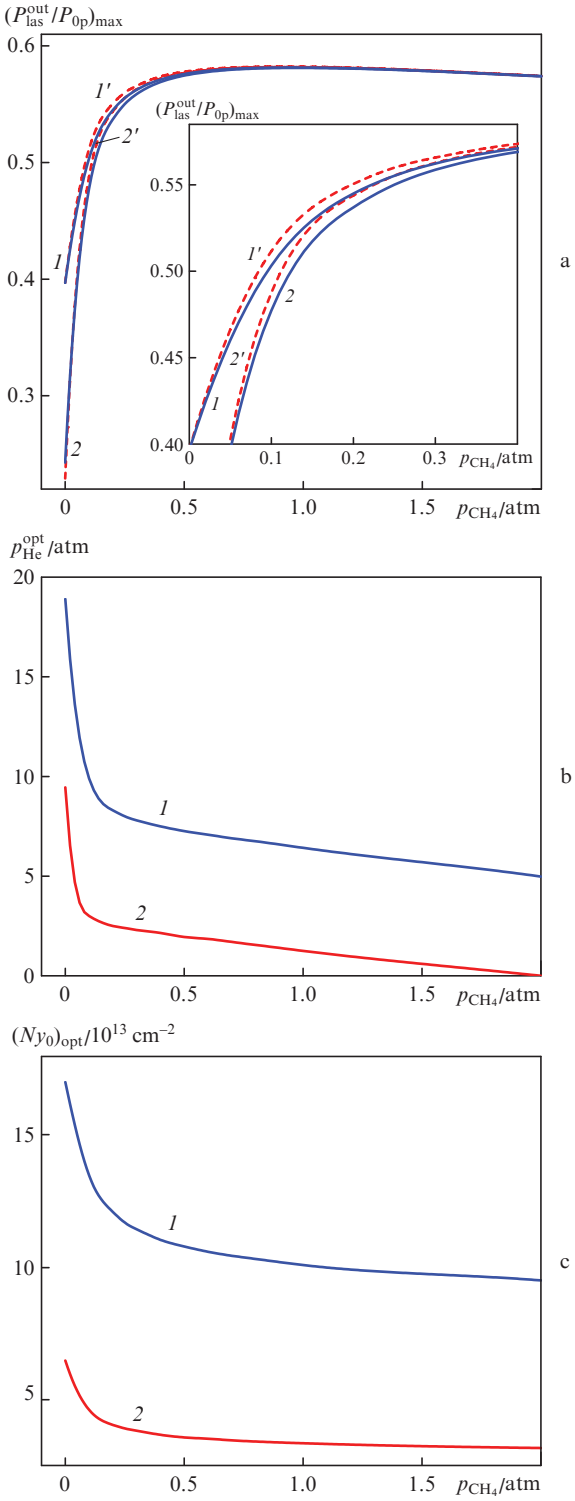

Figure 6. (a) Dependences of the maximum conversion efficiency of pump radiation into laser radiation $(P_{las}^{out}/P_{0p})_{max}$ on the methane pressure p_{CH_4} at optimum parameters of $(Ny_0)_{opt}$ and optimum helium pressures p_{He} [curves (*1′*) and (*2′*) show the results of calculation in the approximation $b = 0$, the calculated parameters are the same as for curves (*1*) and (*2*), respectively; the inset shows on a larger scale the left upper part of Fig. 6a], (b) dependence of the optimum helium pressure p_{He} on the methane pressure p_{CH_4} at optimum parameters of $(Ny_0)_{opt}$ and (c) dependences of the optimum parameter $(Ny_0)_{opt}$ on the methane pressure p_{CH_4} at the optimum helium pressures p_{He}. The calculation parameters are $T = 395$ K, $R_p = 0.99$, $R_0 = 0.3$, $R_1 = 0.99$, $T_0 = 0.99$, $T_1 = 0.99$, $T_s = 0.99$, $\omega_p = \omega_{31}$, $\omega_{las} = \omega_{21}$; (*1*) $I_{0p} = 3$ kW cm^{-2}, $\Delta\omega/(2\pi c) = 3$ cm^{-1} and (*2*) $I_{0p} = 1$ kW cm^{-2}, $\Delta\omega/(2\pi c) = 1$ cm^{-1}.

0.5 atm, the difference between curves (*1*) and (*2*) is so slight that they merge and become indistinguishable by the naked eye].

It can be seen from Figs 6b and 6c that the optimum helium pressure p_{He}^{opt} and the optimal parameter $(Ny_0)_{opt}$ decrease monotonically with increasing methane buffer gas pressure. At the same time, smaller values of the half-width $\Delta\omega$ of the pump radiation spectrum correspond to smaller values of p_{He}^{opt} and $(Ny_0)_{opt}$, which is quite obvious.

Figure 7 illustrates the above statement that for the same spectral power density of pump radiation and optimum values of $(Ny_0)_{opt}$, $p_{CH_4}^{opt}$ and p_{He}^{opt}, the maximum conversion efficiency of pump radiation into laser radiation $(P_{las}^{out}/P_{0p})_{max}$ being the same. For curves (*1*), (*2*), (*3*), (*4*) and (*5*), the spectral output power density is the same $(I_{0p}/[\Delta\omega/(2\pi c)] = 1$ kW cm$^{-1})$ and the same are the maxima of the ratios P_{las}^{out}/P_{0p} (equal to 0.58), which are attained at $p_{He} = 0.7$, 2, 4.6, 7.3 and 10 atm, respectively. At these pressures, the ratio of the half-width $\Delta\omega$ of the pump spectrum to the homogeneous half-width Γ_p of the 3–1 transition line ($\Delta\omega/\Gamma_p = 1.5$) and the ratio $Ny_0/I_{0p} = 3.6\times10^{13}$ kW^{-1} are the same for all the curves.

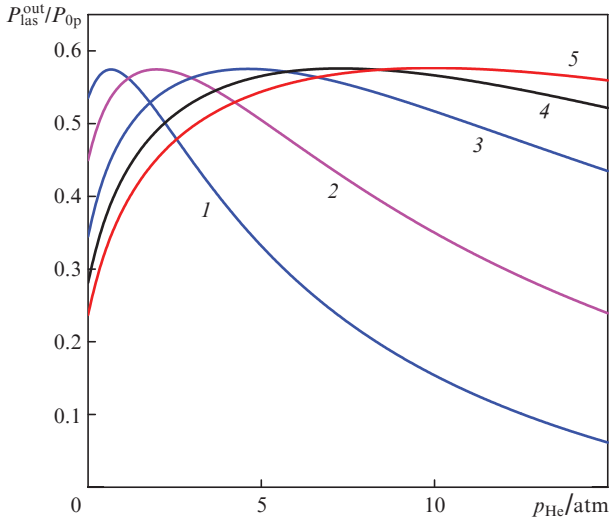

Figure 7. Conversion efficiency of pump radiation into laser radiation as a function of helium buffer gas pressure with the same spectral power density of pump radiation $I_{0p}/\Delta\omega$ and optimal values of $(Ny_0)_{opt}$ and $p_{CH_4}^{opt}$. The calculation parameters are $T = 395$ K, $p_{CH_4} = 0.5$ atm, $R_p = 0.99$, $R_0 = 0.3$, $R_1 = 0.99$, $T_0 = 0.99$, $T_1 = 0.99$, $T_s = 0.99$, $\omega_p = \omega_{31}$, $\omega_{las} = \omega_{21}$; (*1*) $I_{0p} = 0.5$ kW cm^{-2}, $\Delta\omega/(2\pi c) = 0.5$ cm^{-1}, $Ny_0 = 1.8\times10^{13}$ cm^{-2}, (*2*) $I_{0p} = 1$ kW cm^{-2}, $\Delta\omega/(2\pi c) = 1$ cm^{-1}, $Ny_0 = 3.6\times10^{13}$ cm^{-2}, (*3*) $I_{0p} = 2$ kW cm^{-2}, $\Delta\omega/(2\pi c) = 2$ cm^{-1}, $Ny_0 = 7.2\times10^{13}$ cm^{-2}, (*4*) $I_{0p} = 3$ kW cm^{-2}, $\Delta\omega/(2\pi c) = 3$ cm^{-1}, $Ny_0 = 10.8\times10^{13}$ cm^{-2} and (*5*) $I_{0p} = 4$ kW cm^{-2}, $\Delta\omega/(2\pi c) = 4$ cm^{-1}, $Ny_0 = 14.4\times10^{13}$ cm^{-2}.

Figure 8 shows the intensities of laser radiation $I_{las}^{out}(y)/I_{las}^{out}(0)$ and pump radiation $I_p(y)/I_p(0)$ as functions of coordinate y. The intensity profiles were calculated for such parameters of Ny_0 and helium and methane pressures, at which the conversion efficiency of pump radiation into laser radiation P_{las}^{out}/P_{0p} has the highest value. It can be seen that the laser radiation intensity decreases more rapidly with increasing y than the pump radiation intensity. The numerical analysis shows that for a given spectral power density of pump radiation $I_{0p}/\Delta\omega$ but at different $\Delta\omega$ and optimum values of the methane and helium pressures as well as the parameter Ny_0, the intensity profiles of laser radiation and pump radiation do not depend separately on $\Delta\omega$ and I_{0p}.The spectral power density of pump radiation is the same for all the curves in Fig. 7 $(I_{0p}/[\Delta\omega/(2\pi c)] = 1$ kW cm$^{-1})$. At optimum helium pressures (at the points of the curve maxima in Fig. 7), the intensity profiles of laser radiation and pump radiation are described by curves (*1*) and (*2*) in Fig. 8. Each of these curves actually contains five curves with the same parameters as for Fig. 7 and the corresponding optimum helium pressures.

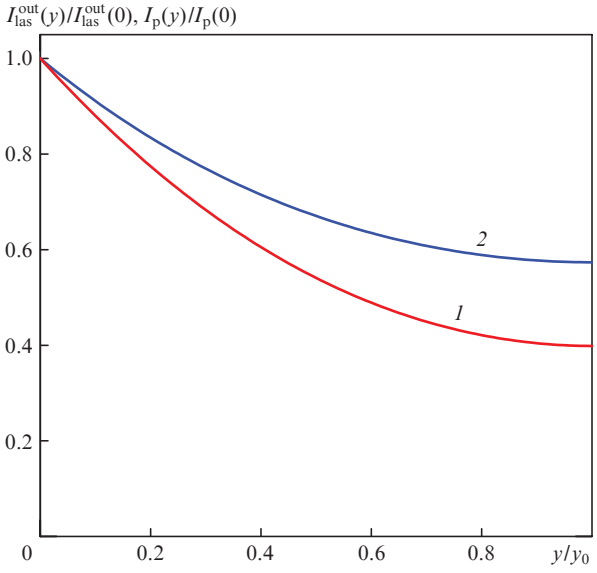

Figure 8. Intensities of (*1*) laser radiation $I_{las}^{out}(y)/I_{las}^{out}(0)$ and (*2*) pump radiation $I_p(y)/I_p(0)$ as functions of the coordinate y with the constant pump power spectral density $I_{0p}/\Delta\omega$ and optimal values of $(N_{y0})_{opt}$, $p_{CH_4}^{opt}$ and p_{He}^{opt}. The calculated parameters are the same as for curves (*1*), (*2*), (*3*), (*4*) and (*5*) in Fig. 7 at points of their maxima for the helium pressure $p_{He} = 0.7$, 2, 4.6, 7.3 and 10 atm, respectively.

Let us compare the results of calculations of the laser energy characteristics obtained numerically in [9] with the results of our calculations using analytical formulas. In considering the possibility of creating a megawatt rubidium vapour laser, Yang et al. [9] used the following parameters of the working medium and pump radiation: $T = 380$ K, $N = 9.34\times10^{12}$ cm^{-3}, $z_0 = 50$ cm, $x_0 = y_0 = 5.5$ cm, $p_{He} = 3.24$ atm, $p_{CH_4} = 0.683$ atm, $I_{0p} = 3.7$ kW cm^{-2}, $\Delta\omega/(2\pi c) = 1.97$ cm^{-1}, $\omega_p = \omega_{31}$, $R_p = 0.99$, $R_0 = 0.3$, $R_1 = 0.99$, $T_0 = 0.99$, $T_1 = 0.99$, $T_s = 0.99$. The influence of the spatial overlap of the laser radiation and pump fields on the lasing efficiency was taken into account in [9] by introducing the parameter $\eta_{mode} = V_{las}/V = 0.96$ (V_{las} is the laser volume in the cell). With these parameters, Yang et al. [9] obtained the conversion efficiency of pump radiation into laser radiation $P_{las}^{out}/P_{0p} = 0.61$ and the ratio of the absorbed pump power to the total pump power $P_{abs}/P_{0p} = 0.725$. The corresponding calculations by our analytical formulas for the same parameters of the working medium and pump radiation yield (after multiplying by $\eta_{mode} = 0.96$) $P_{las}^{out}/P_{0p} = 0.60$, $P_{abs}/P_{0p} = 0.730$. The results of calculations of the laser energy characteristics by analytical formulas are in very good agreement with the results of numerical calculations [9]. Such a good agreement is achieved only when the correction is taken into account for the parameter $b\varkappa_p$. Calculation by simpler analytical formulas in the approximation $b = 0$ gives not so good agreement with the results of

paper [9]: $P_{las}^{out}/P_{0p} = 0.63$, $P_{abs}/P_{0p} = 0.780$. Note that in Ref. [9], not all the parameters of the working medium of a megawatt laser are optimal. According to our calculations, if the concentration of rubidium atoms is increased to 17.8×10^{12} cm^{-3} and the helium pressure is raised to 5.25 atm with the other parameters unchanged, the conversion efficiency will increase to 0.66.

6. Conclusions

We have developed an analytical model of a transversely diode-pumped alkali metal vapour laser, which describes the laser generation in the practically important case of a sufficiently high intensity of laser radiation and with a weak restriction from below on the buffer gas pressure. This restriction is removed by taking into account the correction for the parameter $b\varkappa_p$. In the case of a sufficiently high buffer gas pressure, the parameter $b\varkappa_p$ is very small ($b\varkappa_p \ll 1$) and can be neglected (it can be assumed that $b = 0$) in the equations describing the laser operation. This case was considered earlier in our work [10]. The analytical solution of the differential equations that describe the laser generation makes it possible to determine exhaustively any energy characteristics of the laser and to find the optimum parameters of the working medium and pump radiation (temperature, buffer gas pressure and composition, intensity and width of the pump spectrum).

The conversion efficiency of pump radiation into laser radiation P_{las}^{out}/P_{0p} is described by an analytical formula in which the concentration N of active particles and the cell width y_0 enter only in the combination Ny_0. The efficiency P_{las}^{out}/P_{0p} depends nonmonotonically on the parameter Ny_0, as well as on the pressure of helium p_{He} and methane p_{CH_4} and reaches a maximum value $(P_{las}^{out}/P_{0p})_{max}$ at some optimum parameter $(Ny_0)_{opt}$ and some optimal pressures p_{He}^{opt} and $p_{CH_4}^{opt}$. It is important to note that at the given spectral power density of pump radiation $I_{0p}/\Delta\omega$ and selected optimal values of $(Ny_0)_{opt}$, p_{He}^{opt} and $p_{CH_4}^{opt}$ for different $\Delta\omega$, the lasing efficiency is the same. Calculations using analytical formulas show that the conversion efficiency P_{las}^{out}/P_{0p} reaches 69 % with the spectral power density of pump radiation $I_{0p}/[\Delta\omega/(2\pi c)] = 2$ kW cm^{-1}.

Analytical formulas for intensities of laser radiation $I_{las}^{out}(y)$ and pump radiation $I_p(y)$ are obtained as functions of the coordinate y along the width of the cell. The laser radiation intensity decreases with increasing y faster than the pump radiation intensity. At a given spectral power density of pump radiation $I_{0p}/\Delta\omega$, but for different $\Delta\omega$ and corresponding optimum values of the methane and helium pressures, as well as the parameter Ny_0, the intensity profiles of laser radiation and pump radiation do not depend separately on $\Delta\omega$ and I_{0p}.

Allowance for the correction for the parameter $b\varkappa_p$ can both reduce and increase the calculated values of P_{las}^{out}/P_{0p}. The effect of the correction on the calculated value of P_{las}^{out}/P_{0p} is small for the optimal value of the parameter Ny_0 and becomes significant when Ny_0 deviates from the optimum value. With the optimal value of the parameter Ny_0, the correction for the parameter $b\varkappa_p$ leads to a relative change in the conversion efficiency of pump radiation into laser radiation P_{las}^{out}/P_{0p} by a value that is much smaller than the parameter $b\varkappa_p$ itself. At the same time, the correction for the parameter $b\varkappa_p$ exerts a much stronger effect on the local value of the laser radiation intensity $I_{las}^{out}(y)$. Taking the correction into account leads to a smoother dependence of $I_{las}^{out}(y)$: the intensity decreases from one side of the cell (at $y = 0$) and increases from the other side (at $y = y_0$). The relative changes in intensity near the two sides of the cell have different signs and turn out to be of the order of magnitude of $b\varkappa_p$.

Acknowledgements. The work was supported by the integrated programme of fundamental research of the Siberian Branch of the Russian Academy of Sciences (RAS) (Integration and Development Programme No. II.2P as part of the RAS programme, Project No. II.2P/II.10-13) and RF President's Grants Council (State Support to Leading Scientific Schools Programme, Grant No. NSh-6898.2016.2).

References

1. Krupke F.W. *Progr. Quantum Electron.*, **36**, 4 (2012).
2. Shalagin A.M. *Usp. Fiz. Nauk*, **181**, 1011 (2011).
3. Zhdanov B.V., Knize R.J. *Proc. SPIE Int. Soc. Opt. Eng.*, **8898**, 88980V (2013).
4. Bogachev A.V., Garanin S.G., Dudov A.M., Yeroshenko V.A., Kulikov S.M., Mikaelyan G.T., Panarin V.A., Pautov V.O., Rus A.V., Sukharev S.A. *Quantum Electron.*, **42**, 95 (2012) [*Kvantovaya Elektron.*, **42**, 95 (2012)].
5. Gao F., Chen F., Xie J.J., Li D.J., Zhang L.M., Yang G.L., Guo J., Guo L.H. *Optik*, **124**, 4353 (2013).
6. Krupke W.F., Zweiback J.S., Betin A.A. US Patent No.0022201 Al (2009).
7. Zhdanov B.V., Shaffer M.K., Sell J., Knize R.J. *Opt. Commun.*, **281**, 5862 (2008).
8. Komashko A.M., Zweiback J. *Proc. SPIE Int. Soc. Opt. Eng.*, **7581**, 75810H (2010).
9. Yang Z., Wang H., Lu Q., Li Y., Hua W., Xu X., Chen J. *J. Opt. Soc. Am. B*, **28**, 1353 (2011).
10. Parkhomenko A.I., Shalagin A.M. *Quantum Electron.*, **45**, 797 (2015) [*Kvantovaya Elektron.*, **45**, 797 (2015)].
11. NIST Atomic Spectra Database: https://www.nist.gov/pml/atomic-spectra-database.
12. Rotondaro M.D., Perram G.P. *J. Quant. Spectrosc. Radiat. Transfer*, **57**, 497 (1997).
13. Krause L. *Appl. Opt.*, **5**, 1375 (1966).
14. Hrycyshyn E.S., Krause L. *Can. J. Phys.*, **48**, 2761 (1970).
15. Zameroski N.D., Rudolph W., Hager G.D., Hostutler D.A. *J. Phys. B*, **42**, 245401 (2009).
16. Sell J.F., Gearba M.A., Patterson B.M., Byrne D., Jemo G., Lilly T.C., Meeter R., Knize R.J. *J. Phys. B*, **45**, 055202 (2012).